Heliyon 6 (2020) e03561

Contents lists available at ScienceDirect

Heliyon

journal homepage: www.cell.com/heliyon

Research article

Anti-gastric cancer activity of 1,2,3-triazolo[4,5-d]pyrimidine hybrids (1,2,3-TPH): QSAR and molecular docking approaches

Oyebamiji Abel Kolawole [a,b], Fadare Olatomide A [c], Semire Banjo [b,*]

[a] Department of Basic Sciences, Adeleke University, P.M.B. 250, Ede, Osun state, Nigeria
[b] Computational Chemistry Laboratory, Department of Pure and Applied Chemistry, Ladoke Akintola University of Technology, P.M.B., 4000, Ogbomoso, Oyo State, Nigeria
[c] Organic Chemistry Research Laboratory, Department of Chemistry, Obafemi Awolowo University, Ile-ife, Osun State, Nigeria

ARTICLE INFO

Keywords:
Theoretical chemistry
Pharmaceutical chemistry
1, 2, 3-triazolo[4, 5-d]pyrimidine hybrids
DFT
QSAR
Molecular docking

ABSTRACT

Gastric cancer as a dreaded disease which occurs in the digestive system of human being remain a threat to the medical world. Bioactivity of series of designed and synthesized molecular compounds containing triazole and pyrimidine moieties were subjected to quantum chemical calculations using B3LYP/6-31+G*. The calculated molecular descriptors such as the E_{HOMO} (eV), E_{LUMO} (eV), band gap (eV), chemical hardness (η), global nucleophilicity, dipole moment (Debye), chemical potential, log P, molecular weight (amu) and Ovality. The descriptors that describe anti-gastric cancer activity of the studied compounds were used for QSAR analysis using SPSS and Gretl software packages for multiple linear regression (MLR), XLSTAT for partial least square (PLS) and MATLAB for artificial neural network (ANN). The methods (MLR, PLS, and ANN) were predictive. Nevertheless, ANN performed better than MLR and PLS. More so, molecular docking study was executed on the studied compounds and gastric cancer cell line (**PDB ID:** 4oum); the docking studies showed that 2-(1-(2-(3-benzyl-5-(benzylthio)-3H-[1,2,3]triazolo[4,5-d]pyrimidin-7-yl)hydrazono)ethyl)phenol (**A22**) having the lowest binding affinity (-8.40 kcal/mol); this was correlated to the observed inhibitory activity of the compound against gastric cancer. Thus, it showed better inhibition than other studied compounds. The amino acid residues that were involved in stabilizing **A22** in the active site of the **4oum** are: VAL-9, ALA-10, THR-49, ASN-48, PRO-47 and TYR-46. Also, a good relationship was observed between the calculated binding affinity and the observed inhibition concentration (IC_{50}).

1. Introduction

Cancer remains a dark spot on the outer look of human being in this present century [1]. It still maintains its position as the second cause of death in the entire world [2, 3]. Reichert and Wenger reported cancer to be a chromosomal syndrome which moves through the creation of carcinogenesis with several steps [4]. This malignant neoplasia mostly starts as a restrained illness. However, it spreads all over the human body with time [5]. More so, elongated cough, weight loss, unusual bleeding and swellings are possible signs of cancer in the body [6, 7].

Moreover, gastric cancer is a usual menace that occurs in the digestive system of a human being [8]. It has been rated to be the fifth cause of death in the entire world and the third in cancer-related death [9, 10]. It mostly occurs in places like South America, eastern Asia, as well as Eastern Europe. Gastric cancer affects male much more than female and over 900000 new issues are reported every year [11, 12]. Several measures have been attempted over the years to combat gastric cancer in the human race like combination of chemotherapy, surgical resection, and radiation protocols; none of the curative means has been established [13].

The role played by heterocycle in the discovery and development of novel drugs is imperative. 1, 2, 3-triazolo[4, 5-d]pyrimidine derivatives as heterocyclic molecules comprise of two active compounds (triazole and pyrimidine moieties). These are good class of compounds with renown biological activities which has drawn the attention of medicinal community in their exploration as anti-inflammatory [14, 15], anticancer [16], antimicrobial [17, 18], diuretics [19], analgesics [20, 21], antioxidant [22].

Growing interest of researchers to develop a prediction method for biological activities before synthesis in recent times is becoming

* Corresponding author.
E-mail address: bsemire@lautech.edu.ng (S. Banjo).

https://doi.org/10.1016/j.heliyon.2020.e03561
Received 6 February 2020; Received in revised form 1 March 2020; Accepted 4 March 2020

alarming. Therefore, quantitative structure–activity relationship (QSAR) helps in searching information connecting chemical structure/molecular properties to biological and other activities by developing a QSAR model. This approach can be used to predict the activities of newly designed compounds before synthesis. The scope of designing drugs and examining the process of drug activities have been widened through recent developments in QSAR studies [23]. Several methods (heuristic method (HM), partial least squares (PLS), multiple linear regression (MLR), genetic algorithm (GA) and various types of artificial neural networks (ANN)) can be used for developing QSAR model which has brought advancement in QSAR studies [24].

Therefore, thirty-two compounds as shown in Figure 1 were optimized using density functional theory in order to obtain molecular parameters. Twenty-two compounds (**A1-A22**) from the entire compounds used in this work were taken form Li *et al.*, (2016) [25], five compounds (**A23-A28**) were also taken from Li *et al.*, (2017) and the last set of compounds were taken from the work of Geng *et al.*, 2018. The anticancer activities of all these compounds had been experimentally reported [26, 27]; however, correlation between the molecular properties and anti-gastric cancer activity of 1,2,3-triazolo[4,5-d]pyrimidine hybrids have not been established. Also, the binding affinities of these compounds through molecular docking with gastric cancer cell line which can help in understanding pharmacokinetics and pharmacodynamics of drugs is yet to be established. This is also become imperative to understand the binding mode and non-bonding interactions between the compound's and the amino acid residues involved in the interaction. Therefore, the main objective of this work is to develop QSAR models through multiple linear regression, MLR (via ordinary least squares (OLS) and partial least squares (PLS)) and artificial neural network (ANN) form the calculated molecular descriptors of 1,2,3-triazolo[4,5-d]pyrimidine Hybrids. Also, to probe into non-bonding interactions in terms of affinity, hydrophilic interactions and hydrophobic interactions between these compounds and the gastric cancer cells line (**PDB ID:** 4oum) downloaded from protein data bank [28] via molecular docking.

2. Methodology

Due to the flexibility of the rotatable bonds in these compounds, conformational search was performed on these compounds using semi-empirical AM1 method Monte Carlo search algorithm to select best conformer suitable for optimization. Five hundred (500) conformers were examined for each conformational search and the lowest-energy conformer of this conformational search was taken for further DFT calculations. Density functional theory method of B3LYP with 6-31+G* as basis set was used for optimization of 1, 2, 3-triazolo[4, 5-d]pyrimidine derivatives in gas phase and the energy calculation in water using Spartan 14 [29]. The obtained molecular descriptors such as the highest occupied molecular orbital energy (E_{HOMO}), the lowest unoccupied molecular orbital energy (E_{LUMO}), band gap (eV), chemical hardness (η), global nucleophilicity, dipole moment (Debye), chemical potential (μ), log P, molecular weight (amu) and Ovality were extracted and used to develop Quantitative structural activities relationship (QSAR) models (Table 1). This was accomplished via SPSS/Gretl for multiple linear regression (Ordinary least square), XLSTAT [30] for partial least square and MATLAB for the artificial neural network (ANN). The multiple linear regression reveals the correlation between the dependent variable and some independent variables. It is also used to select the parameters that are used for partial least square and artificial neural network. The developed QSAR models were validated by using statistical analysis such as correlation coefficient (R), adjusted correlation coefficient R^2_{adj}, cross-validation (CVR^2) (Eqs. (1) and (2)) and the significance level (p-value) [31] and the calculated variation inflation factors (VIF) which helps in detecting Multi-collinearity in QSAR analysis (Eq. (3)) [32]. Furthermore, docking study was carried out to predict the binding affinity and calculate equilibrium constant (Ki) using Eq. (4), and also to

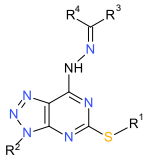

Compounds	R^1	R^2	R^3	R^4
A1	Propyl	Bn	2-Cl-Ph	H
A2	Propyl	Bn	3,4,5-triMeO-Ph	H
A3	Propyl	Bn	4-NO_2-Ph	H
A4	Propyl	Bn	4-(N,N-diMe)-Ph	H
A5	Propyl	Bn		H
A6	Propyl	Bn		H
A7	Propyl	Bn	2-OH-Ph	CH_3
A8	Propyl	Bn	4-OH-Ph	CH_3
A9	Propyl	Bn	4-Br-Ph	CH_3
A10	Propyl	3-Cl-Bn	2-OH-Ph	CH_3
A11	Propyl	4-Cl-Bn	2-OH-Ph	CH_3
A12	Propyl	4-Br-Bn	2-OH-Ph	CH_3
A13	Propyl	4-F-Bn	2-OH-Ph	CH_3
A14	Propyl		2-OH-Ph	CH_3
A15	Propyl		2-OH-Ph	CH_3
A16	Propyl	4-OH-Bn	2-OH-Ph	CH_3
A17	Propargyl	Bn	3,4,5-triMeO-Ph	H
A18	Propargyl	Bn		H
A19	Propargyl	Bn	4-(N,N-diMe)-Ph	H
A20	Propargyl	Bn	2-OH-Ph	CH_3
A21	Bn	Bn	3,4,5-triMeO-Ph	H
A22	Bn	Bn	2-OH-Ph	CH_3

R

A23	4-(n-Butyl)-Ph
A24	2-Pyridyl
A25	3-Pyridyl
A26	Bn
A27	
A28	

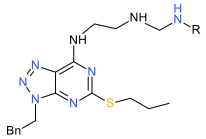

	R^1	R^2	R^3
A29	Propyl	Bn	Bn
A30	Propyl		Bn
A31	propargyl	Bn	Bn
A32	Bn	Bn	Bn

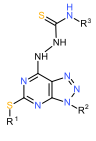

Figure 1. The schematic structures of 1,2,3-triazolo[4, 5-d]pyrimidine analogues.

Table 1. Pearson's correlation matrix for calculated parameters.

	MGC803	E_{HOMO}	E_{LUMO}	PSA	HBA	CON/n	N4	N5	NOR	NOH	VIF
MGC803	1.000										-
HOMO	0.296	1.000									1.548
LUMO	0.430	0.223	1.000								3.462
PSA	-0.139	-0.036	0.336	1.000							2.281
HBA	0.167	0.253	0.226	0.543	1.000						8.506
CON/n	-0.240	-0.162	-0.136	0.039	-0.332	1.000					3.182
N4	-0.083	-0.131	-0.096	0.093	-0401	0.203	1.000				1.641
N5	0.252	-0.101	0.494	0.080	-0.299	0.608	0.008	1.000			4.980
NOR	0.088	0.022	0.190	0.495	0.867	-0.170	-0.364	-0.155	1.000		5.372
NOH	-0.414	0.180	-0.116	0.066	0.035	0.020	-0.006	-0.025	-0.070	1.000	1.139

observe other non-bonded interactions between the studied ligands/-compounds and the gastric cancer cells line (**PDB ID:** 4oum).

$$CV.R^2 = 1 - \frac{\sum (Y_{obs} - Y_{cal})^2}{\sum (Y_{obs} - \overline{Y}_{obs})^2} \quad (1)$$

The adjusted R^2 could be calculated using Eq. (2)

$$R_a^2 = \frac{(N - I) \times R^2 - P}{N - 1 - P} \quad (2)$$

$$VIF = \frac{1}{1 - R^2} \quad (3)$$

$$\Delta G^{\circ} = -RTln\ K_i \quad (4)$$

Table 2. Calculate descriptors from 1,2,3-triazolo[4,5-d]pyrimidine derivatives.

	HOMO	LUMO	PSA	HBA	CON/n	N4	N5	NOR	NOH	MGC-803
A1	-6.68	-2.74	53.122	7	-0.189	0.011	0.28	9	4	10.91
A2	-6.44	-2.55	81.433	10	-0.165	-0.078	0.261	11	4	9.41
A3	-5.88	-2.41	107.577	10	-0.211	0.07	0.238	11	4	10.05
A4	-5.66	-2.47	60.796	8	-0.178	-0.054	0.264	9	4	13.14
A5	-5.92	-2.47	69.208	8	-0.252	0.126	0.175	9	5	7.41
A6	-6.13	-2.67	72.457	8	-0.219	0.119	0.228	9	5	3.71
A7	-6.44	-2.39	76.777	8	-0.209	0.098	0.263	9	4	2.31
A8	-6.36	-2.42	78.887	8	-0.23	0.096	0.239	9	4	16.72
A9	-6.54	-2.49	59.086	7	-0.227	0.104	0.237	9	4	6.02
A10	-6.62	-2.6	73.549	8	-0.243	0.069	0.239	10	4	6.50
A11	-6.45	-2.41	76.777	8	-0.221	-0.004	0.278	10	4	7.10
A12	-6.47	-2.43	76.777	8	-0.222	0.005	0.286	10	4	11.28
A13	-6.42	-2.37	76.777	8	-0.222	0.072	0.277	10	4	10.98
A14	-6.57	-2.59	81.072	9	-0.244	0.072	0.172	10	4	4.76
A15	-6.63	-2.59	73.634	9	-0.238	0.041	0.209	10	4	16.38
A16	-6.42	-2.36	96.667	9	-0.215	0.133	0.265	10	4	7.68
A17	-6.49	-2.65	81.433	10	-0.169	-0.007	0.241	13	4	4.67
A18	-6.13	-2.71	72.457	8	-0.218	0.121	0.209	9	5	10.51
A19	-5.67	-2.55	60.796	8	-0.178	0.028	0.25	9	4	7.62
A20	-6.65	-2.63	73.398	8	-0.24	-0.008	0.239	9	4	3.82
A21	-6.45	-2.57	81.433	10	-0.164	-0.079	0.253	11	5	1.32
A22	-6.44	-2.38	76.772	8	-0.215	-0.046	0.264	9	5	0.85
A23	-5.99	-2.31	66.518	9	-0.23	-0.02	0.408	10	4	31.20
A24	-6.19	-2.29	75.701	10	-0.292	0.156	0.102	11	4	11.55
A25	-6.19	-2.33	73.258	10	-0.31	-0.137	0.129	11	4	16.37
A26	-6.05	-2.28	67.971	9	-0.27	-0.084	0.267	10	4	17.42
A27	-6.17	-2.21	74.31	10	-0.285	-0.118	0.235	11	4	19.22
A28	-5.82	-2.25	86.393	11	-0.317	-0.136	0.16	12	5	9.21
A29	-6.22	-2.82	66.81	9	-0.285	0.049	0.019	10	4	10.42
A30	-6.21	-2.65	70.955	9	-0.254	0.1	0.088	10	3	16.65
A31	-6.24	-2.89	66.386	9	-0.293	-0.252	0.053	10	4	2.37
A32	-6.23	-3.02	67.893	9	-0.256	0.087	0.061	10	5	2.88

3. Results and discussion

The optimization of 1,2,3-triazolo[4,5-d]pyrimidine Hybrids brought about several descriptors that describe anti-gastric cancer activities, but few were selected through Pearson correlation which was used to correlate the individual descriptor to the inhibition concentration (IC_{50}). The selected descriptors were E_{HOMO}, the E_{LUMO}, polar surface area (PSA), Log P, Ovality and heteroatoms as displayed in Table 2. As shown in Table 1, there was a fair correlation between the calculated descriptors; hydrogen bond acceptor (HBA) is correlated with polar surface area by 0.543; electronic charge on nitrogen atom (5) is correlated with average of charge on all nitrogen atoms in 1,2,3-triazolo[4,5-d]pyrimidine derivatives by 0.608. Also, number of rings in the studied compounds is correlated with HBA by 0.867. Thus, Pearson correlation played a decisive role in the selection of descriptors that can describe the bioactivity of compounds.

Moreover, the calculated variation inflation factors (VIF) which help in detecting multi-collinearity in QSAR analysis were all less than 5 in this work, which show that the selected descriptors were not collinearized.

3.1. QSAR study using multiple linear regression (MLR)

The QSAR model obtained using multiple linear regression via ordinary least square (OLS) was shown in Eq. (5). Several descriptors were chosen to show the relationship between the observed IC_{50} (MGC-803; **PDB ID** 4oun) and the selected independent variables i.e., Hydrogen Bond Acceptor (HBA), NOH (Number of Heteroatom), N5, N4, Polar Surface Area (PSA), NOR (Number of Rings), CON/n (Table 2). The obtained equation using MLR is:

$$IC_{50} = -8.24612 + 7.09745(HBA) - 5.62245(NOH) + 67.3318(N5) + 22.8898(N4) - 0.352905(PSA) - 2.79441(NOR) - 80.0762\left(CON/_n\right) \quad (5)$$

$N = 32$, $F = 8.02$, $P < 0.0001$, $R^2 = 0.700$, $R^2_{adj} = 0.613$, $C.VR^2 = 0.902$, $MSE = 1.205$.

The developed model revealed that HBA, N5, and N4 contributed positively to the studied bioactivity while NOH, PSA, NOR and CON/n contributed negatively. As reported by Taourati *et al.*, (2017), the reliability of the developed QSAR model is a function of greater correlation coefficient (R^2), i.e., ≥ 0.5 [33]. The value obtained for R^2, adjusted R^2 and calculated cross-validation, $C.VR^2$, showed that the developed model using MLR has a good predictability, and it is statistically acceptable, since the value for adjusted $R^2 \geq 0.6$ which is the standard and $C.VR^2$ is greater than the standard (0.5) [34]. The R^2 showed that the fitness of the predicted bioactivity to the observed bioactivity is reasonable and it is dependable (Figure 2).

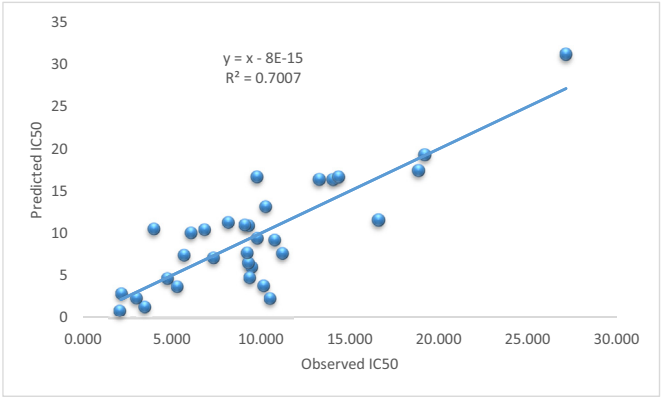

Figure 2. The calculated predicted IC_{50} against the observed IC_{50} using MLR via OLS.

3.2. QSAR study using partial least square (PLS)

Quantitative evaluation of derivatives attached to 1, 2, 3-triazolo[4,5-d]pyrimidine by enhancing structural-activity-relationship were also observed using partial least square. The calculated descriptors which described the anti-gastric cancer activity of 1, 2, 3-triazolo[4,5-d]pyrimidine and its derivatives using MLR were subjected to PLS analysis. Thirty-two molecular compounds were used as a training set, and correlation coefficient (R^2), adjusted R^2 and calculated cross-validation ($C.VR^2$) were used for evaluation, and validation of the developed model (Eq. (6)). The role played by the selected descriptors in the developed model are highly imperative and these were graphically displayed in Figure 3.

$$IC_{50} = -8.241 - 0.352*PSA + 7.097*HBA - 80.050*CON/_n + 22.887*N4 + 67.324*N5 - 2.795*NOR - 5.623*NOH \quad (6)$$

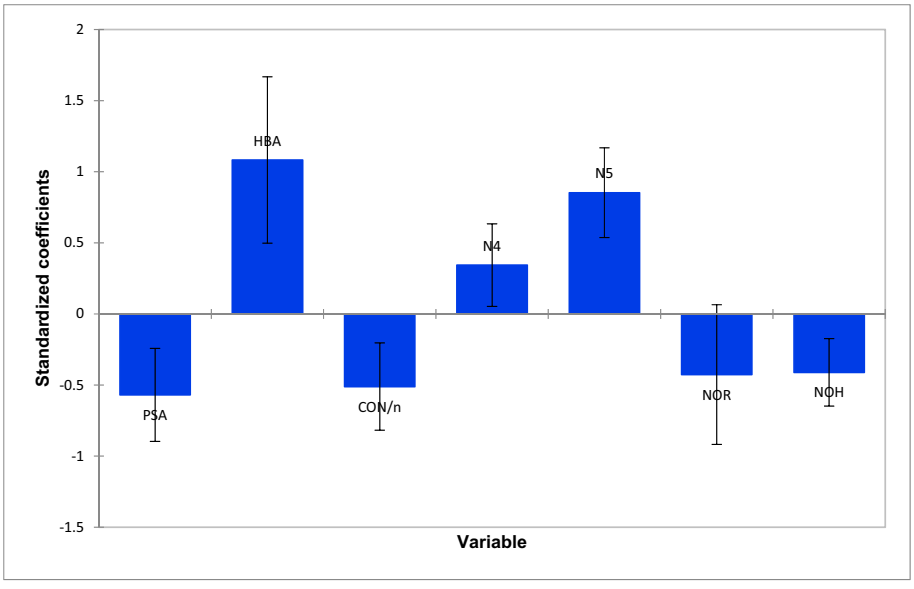

Figure 3. Graphical representation of the coefficient against the independent variables.

Table 3. Stepwise regression result for anti-gastric cancer activity.

	Obs. IC_{50}	OLS-MLR	Residual	PLS-MLR	Residual	ANN-MLR	Residual
A1	10.91	9.29	1.62	9.287	1.623	10.885	0.02
A2	9.41	9.76	-0.35	9.766	-0.356	9.382	0.02
A3	10.05	6.07	3.98	6.064	3.986	10.046	0.00
A4	13.14	10.23	2.91	10.232	2.908	13.112	0.02
A5	7.41	5.69	1.72	5.693	1.717	7.391	0.01
A6	3.71	5.31	-1.6	5.313	-1.603	3.707	0.00
A7	2.31	10.49	-8.18	10.488	-8.178	2.301	0.00
A8	16.72	9.76	6.96	9.763	6.957	16.703	0.01
A9	6.02	9.46	-3.44	9.459	-3.439	5.991	0.02
A10	6.5	9.27	-2.77	9.274	-2.774	6.471	0.02
A11	7.1	7.33	-0.23	7.329	-0.229	7.095	0.00
A12	11.28	8.15	3.13	8.153	3.127	11.25	0.02
A13	10.98	9.08	1.9	9.081	1.899	10.95	0.02
A14	4.76	9.35	-4.59	9.355	-4.595	4.74	0.01
A15	16.38	13.28	3.1	13.281	3.099	16.35	0.02
A16	7.68	9.19	-1.51	9.190	-1.510	7.67	0.00
A17	4.67	4.77	-0.1	4.774	-0.104	4.65	0.01
A18	10.51	4.00	6.51	4.000	6.510	10.48	0.02
A19	7.62	11.17	-3.55	11.166	-3.546	7.59	0.02
A20	3.82	10.12	-6.3	10.119	-6.299	3.79	0.02
A21	1.32	3.5	-2.18	3.501	-2.181	1.3	0.01
A22	0.85	2.12	-1.27	2.118	-1.268	0.84	0.00
A23	31.2	27.15	4.05	27.152	4.048	31.17	0.02
A24	11.55	16.61	-5.06	16.605	-5.055	11.52	0.02
A25	16.37	14.02	2.35	14.020	2.350	16.34	0.02
A26	17.42	18.89	-1.47	18.884	-1.464	17.39	0.02
A27	19.22	19.22	0.00	19.219	0.001	19.19	0.02
A28	9.21	10.74	-1.53	10.736	-1.526	9.19	0.01
A29	10.42	6.84	3.58	6.842	3.578	10.4	0.01
A30	16.65	14.33	2.32	14.334	2.316	16.64	0.00
A31	2.37	3.03	-0.66	3.032	-0.662	2.34	0.02
C32	2.88	2.21	0.67	2.213	0.667	2.87	0.00

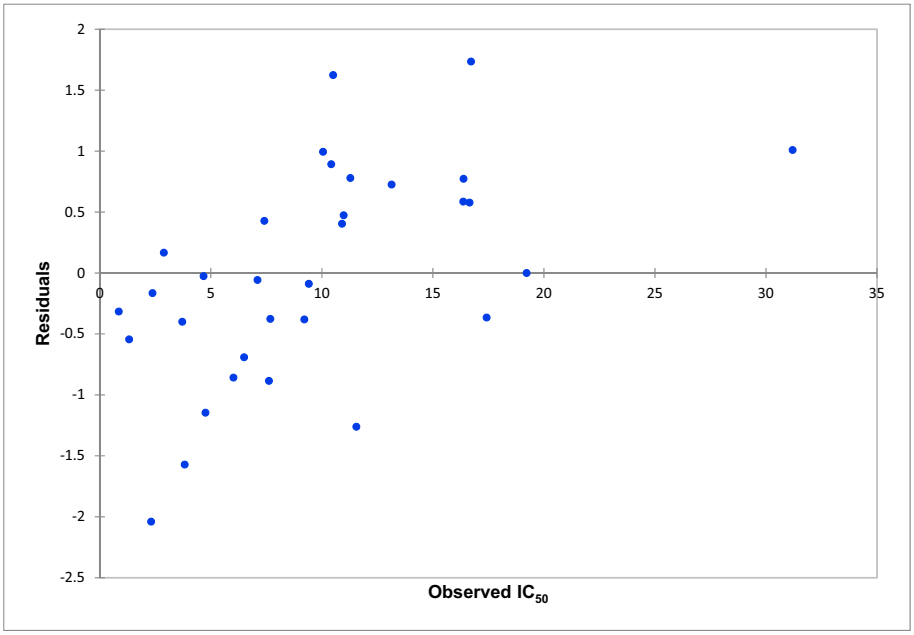

Figure 4. The residuals against observed IC_{50}.

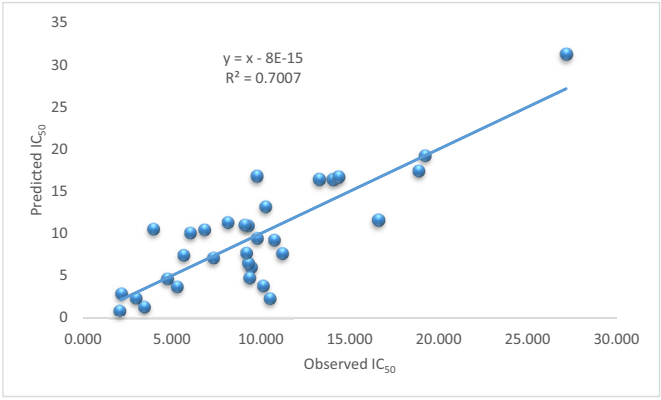

Figure 5. The calculated predicted IC_{50} against the observed IC_{50} using multiple non-linear regression method.

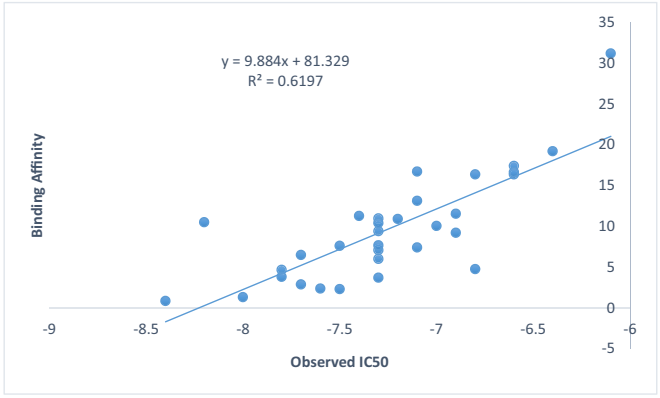

Figure 7. Correlation between Binding affinity and Observed IC_{50}.

N = 32, R^2 = 0.701, R^2_{adj} = 0.613, C.VR^2 = 0.902, F = 8.028, P < 0.0001, MSE = 16.078.

The observed statistical values for PLS showed that the developed model is dependable and predictive as shown in Table 3. Also, the indiscriminate spread of the residuals on the two sides of zero as shown in Figure 4 revealed that the developed model did not display any relative inaccuracy. The calculated R^2 for PLS revealed that the predicted IC_{50} fitted well with observed IC_{50} which shows the dependability of the developed model (Figure 5).

3.3. Artificial neural network (ANN)

Artificial neural network via back propagation neural network (BPNN) has been a veritable tool in developing a predictive and efficient QSAR model [35]. It was used to establish the structural activity relationship between the selected descriptors from MLR and the experimental IC_{50}.

The obtained R^2 (0.999) and MSE (0.24) for BPNN show its effectiveness in prediction than MLR and PLS (Table 2). According to Taourati et al., 2017 [33], reliable and predictive QSAR model is a function of higher correlation coefficient (R^2) and lower mean squared errors; thus, back propagation neural network has proved to be a veritable tool in developing QSAR model with efficient predictability (Figure 6).

3.4. Molecular docking study

A way of recognising pharmacophore with the capacity to interconnect with an enzyme which is a function of binding affinity defines

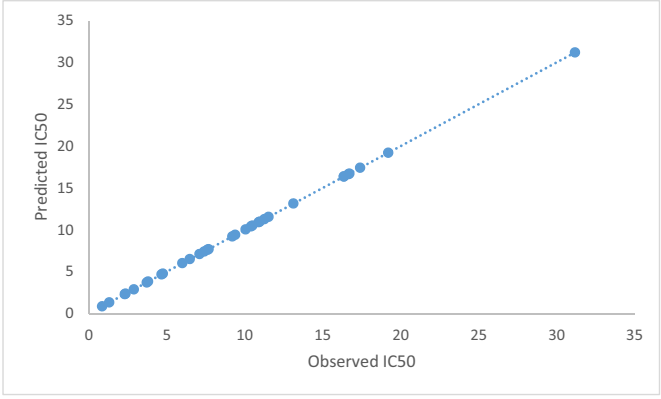

Figure 6. Graphical illustration of predicted and observed bioactivity using artificial neural network method.

docking study. According to Ritchie *et al.*, 2008, the impulsiveness of the binding relationship between ligand and the studied enzyme could be improved by lowering of binding energy [36]. Therefore, the summary of the docking results showing in Table 3, indicated that the affinity calculated for **A22** was -8.40 kcal/mol. This was in line with observed inhibitory activity of **A22** against gastric cancer cell line as a compound with highest inhibition. This can be due to the benzyl groups at R^1 and R^2 positions in **A22** which give rise to amide-π stacking in addition to other interactions in the active gorge of the receptor. The relationship between the cytotoxicity and affinity was displayed in Figure 7. For concise understanding of the docked results, five ligand-receptor complexes were selected and analysed vis-à-vis **A17, A18, A20, A21 and A22** docked with receptor. The amino acid residues involved in hydrophobic interactions (HIs) with **A17, A18, A20, A21** and **A22** with **4oum** are ARG-1004, VAL-1018, LEU-1034 and PRO-1016 for **A17**; PRO-1010, PRO-1016, LEU-1034, VAL-1018, ARG-1004 for **A18**; ASP-1020, ARG-1004, LEU-1008, PRO-1010, VAL-1018, LEU-1032 for **A20**; VAL-1018, ARG-1004, ASP-1020, LEU-1032, GLN-1033 for **A21**, and VAL-1018, ARG-1004, ASP-1020, LEU-1032 and GLN-1033 for **A22** (Figure 8). Comparing these compounds with the standard drug, 5-Fu, it was observed that all the studied compounds in this work inhibited more effectively and also have lower affinity (<-4.30 kcal/mol and $K_i > 1.42 \times 10^3$) than the standard compound used (5-FU) as shown in Table 4. Therefore, the combination of both triazole and pyridine moieties would prove to be a very good architecture in designing potent drugs that will be effective inhibit gastric cancer than 5-FU. The residues involve in the interactions between 5-FU and 4oum are PHE-1019, ARG-1004, and VAL-1018 and the inhibition constant (K_i) was very low compared to the values obtained for other studied compounds, a function of the calculated binding affinity.

4. Conclusion

Bioactivity of 32 sets of 1, 2, 3-triazolo[4, 5-d]pyrimidine derivatives was studied by observing the calculated electronic descriptors using density functional theory method via 6-31+G(d,p) as a basis set. The selected molecular descriptors after optimization of these of 1, 2, 3-triazolo[4, 5-d]pyrimidine analogues were used to develop QSAR models for anti-gastric cancer activity. The methods used (MLR, PLS, and ANN) were predictive. However, ANN prediction is more effective than other methods used in this study. Also, the molecular docking study was conducted to reveal the binding interactions between the studied compounds and the receptor. The results showed that 2-(1-(2-(3-benzyl-5-(benzylthio)-3H-[1,2,3]triazolo[4,5-d]pyrimidin-7-yl)hydrazono)ethyl) phenol (**A22)** presented lowest affinity and highest inhibitory activity than other compounds; thus most promising drug-like compound for gastric cancer inhibition.

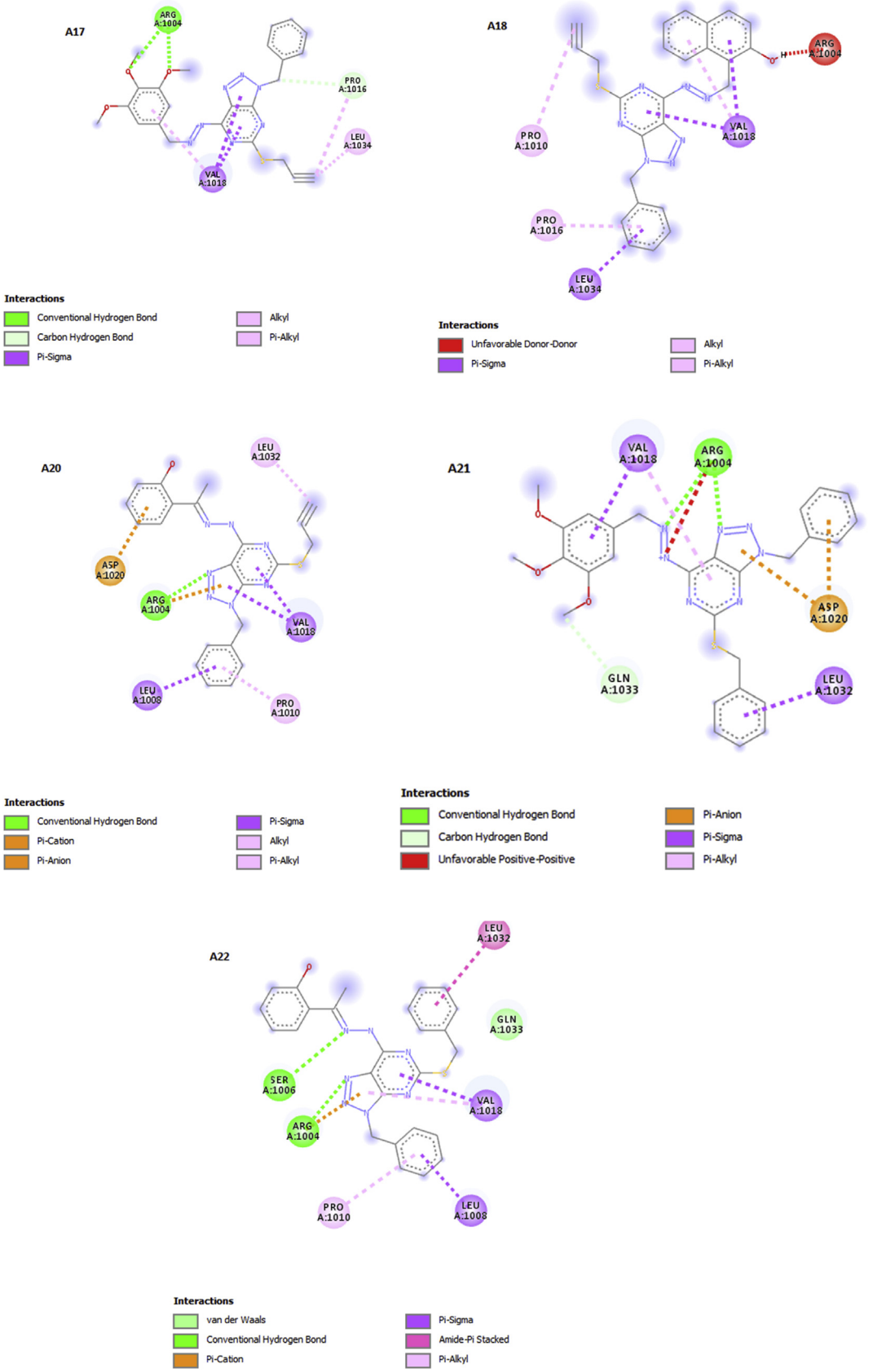

Figure 8. Molecular binding interaction between A17, A18, A20, A21, and A32 with 4oum.

Table 4. Interactions between ligands and 4oum receptor.

Comp	Scoring	K	Hydrogen Bonds	Amino Acid Residues
A1	-7.2	1.90913×10^5	-	
A2	-7.3	2.26037×10^5	(i) ARG-1004, LIG: O (ii) ARG-1004, LIG: O	VAL-1018, PRO-1016, LEU-1034, GLY-1011, PRO-1010
A3	-7.0	1.36190×10^5	(i) ARG-1004, LIG:N (ii) i) ARG-1004, LIG:N	ASP-1020, LUE-1008 PRO-1010, VAL-1018
A4	-7.1	1.61246×10^5	(i) ARG-1004, LIG:N (ii) ARG-1004, LIG:N	VAL-1018, LUE-1008, PRO-1010
A5	-7.1	1.61246×10^5	(i) PRO-1004, LIG:H (ii) ARG-1004, LIG:N	VAL-1081, PRO-1016, ARG-1004
A6	-7.3	2.26037×10^5	-	PRO-1016, VAL-1018, LEU-1034, GLY-1011, PRO-1010
A7	-7.5	3.16862×10^5	ARG-1004, LIG:N	ASP-1020, ARG-1004, LEU-1008, PRO-1010, VAL-1018, LEU-1032
A8	-7.1	1.61246×10^5	(i) ARG-1004, LIG:N (ii) ARG-1004, LIG:N (iii) GLN-1033	LEU-1032, GLN-1032, VAL-1018, PRO-1010, LEU-1008, ARG-1004
A9	-7.3	2.26037×10^5	(i) ARG-1004, LIG: N (ii) ARG-1004, LIG: N (iii) ARG-1004, LIG: N	ARG-1004, PRO-1016, ASP-1020
A10	-7.7	4.44181×10^5	ARG-1004, LIG: N	VAL-1018, PRO-1010, LEU-1008, ARG-1004
A11	-7.3	2.26037×10^5	ASP-1020, LIG:O (ii) ARG-1004, LIG:O	ASP-1020, ARG-1004
A12	-7.4	2.67624×10^5	SER-1006, LIG:N (ii) ARG-1004, LIG:N	SER-1006, ARG-1004
A13	-7.3	2.26037×10^5	-	PRO-1010, PRO-1016, VAL-1018,
A14	-6.8	9.715×10^4	(i)ASP-1020, LIG:H (ii) ARG-1004, LIG-O	ASP-1020, ARG-1004, VAL-1018, LEU-1008, PRO-1010
A15	-6.8	9.715×10^4	(i) SER-1006, LIG:N (ii) ARG-1004, LIG:N (iii) ARG-1004, LIG:N	SER-1006, ARG-1004,ASP-1020, VAL-1018, LEU-1008, PRO-1010
A16	-7.3	2.26037×10^5	(i) ARG-1004, LIG:N (ii) ARG-1004, LIG:N	ARG-1004, VAL-1018, LEU-1032
A17	-7.8	5.25902×10^5	(i) ARG-1004, LIG:O (ii) ARG-1004, LIG:O	ARG-1004, VAL-1018, LEU-1034, PRO-1016
A18	-8.2	1.033440×10^6	-	PRO-1010, PRO-1016, LEU-1034, VAL-1018, ARG-1004
A19	-7.5	3.16862×10^5	(i) ARG-1004, LIG:N (ii) ARG-1004, LIG:N	ARG-1004, VAL-1018, ASP-1020, LEU-1032
A20	-7.8	5.25902×10^5	ARG-1004, LIG:N	ASP-1020, ARG-1004, LEU-1008, PRO-1010, VAL-1018, LEU-1032
A21	-8.0	7.37217×10^5	(i) ARG-1004, LIG:N (ii) ARG-1004, LIG:N	VAL-1018, ARG-1004, ASP-1020, LEU-1032, GLN-1033
A22	-8.4	1.448689×10^6	(i) SER-1006, LIG:N (ii) ARG-1004, LIG: N	SER-1006, ARG-1004, PRO-1010, LEU-1008, VAL-1018, GLN-1033, LEU-1032
A23	-6.1	2.9788×10^4	(i) PHE-1019, LIG:S (ii) ARG-1004, LIG:H (iii) ARG-1004, LIG:N	PHE-1019, ARG-1004,
A24	-6.9	1.15027×10^5		
A25	-6.6	6.9305×10^4	(i) ARG-1004, LIG: N	ARG-1004, LEU-1008, PRO-1010 and VAL-1018
A26	-6.6	6.9305×10^4	(i) ASN-1007, LIG:H (ii) SER-1006, LIG:N	PRO-1010, LEU-1008, ASN-1007, VAL-1018, SER-1006 and ARG-1004
A27	-6.4	4.9439×10^4	(i) ARG-1004, LIG: N	VAL-1018, LEU-1032, ARG-1004, PRO-1010 and LEU-1008
A28	-6.9	1.15027×10^5	(i) ARG-1004, LIG: N	ARG-1004, VAL-1018, PRO-1016, ASN-1007 and LEU-1032
A29	-7.3	2.26037×10^5	(i) ARG-1004, LIG: N (ii) ARG-1004, LIG: N	LEU-1008, PRO-1010, ARG-1004, VAL-1018, and LEU-1032
A30	-6.6	6.9305×10^4	(i) ARG-1004, LIG: N (ii) ARG-1004, LIG: N	LEU-1008, PRO-1010, VAL-1018, LEU-1032 and ARG-1004
A31	-7.6	3.75159×10^5	(i) ARG-1004, LIG: N (ii) ARG-1004, LIG: N	LEU-1008, PRO-1010, VAL-1018, LEU-1032 and ARG-1004
A32	-7.7	4.44181×10^5	(i) ARG-1004, LIG: N (ii) ARG-1004, LIG: N	PRO-1010, LEU-1008, VAL-1018, ARG-1004 and LEU-1032

Declarations

Author contribution statement

Banjo Semire: Conceived and designed the experiments.

Fadare O A: Analyzed and interpreted the data.

Oyebamiji Abel K: Conceived and designed the experiments; Performed the experiments; Analyzed and interpreted the data; Contributed reagents, materials, analysis tools or data; Wrote the paper.

Funding statement

This research did not receive any specific grant from funding agencies in the public, commercial, or not-for-profit sectors.

Competing interest statement

The authors declare no conflict of interest.

Additional information

No additional information is available for this paper.

References

[1] Imran Ali, Mohammad Nadeem L., Haasan Y. Aboul-Enein, Imidazoles as potential anticancer agents, Med. Chem. Commun. 8 (2017) 1742–1773.

[2] J.Y. Zhang, Apoptosis-based anticancer drugs, Nat. Rev. Drug Discov. 1 (2002) 101–102.

[3] J.K. Buolamwini, Novel anticancer drug discovery, Curr. Opin. Chem. Biol. 3 (1999) 500–509.

[4] J.M. Reichert, J.B. Wenger, Development trends for new cancer therapeutics and vaccines, Drug Discov. Today 13 (1–2) (2008) 30–37.

[5] J.R. Molina, P. Yang, S.D. Cassivi, S.E. Schild, A.A. Adjei, Non-small cell lung cancer: epidemiology, risk factors, treatment, and survivorship, in: Mayo Clinic Proceedings, Elsevier, 2008, pp. 584–594.

[6] R. Kumar, R. Srivastava, S. Srivastava, Detection and classification of cancer from microscopic biopsy images using clinically significant and biologically interpretable features, J. Med. Eng. (2015) 14. Article ID 457906.

[7] C.S. Grasso, Y.M. Wu, D.R. Robinson, X. Cao, S.M. Dhanasekaran, A.P. Khan, M.J. Quist, X. Jing, R.J. Lonigro, J.C. Brenner, The mutational landscape of lethal castration-resistant prostate cancer, Nature 487 (7406) (2012) 239–243.

[8] Wenting Xu, Zhen Yang, Nonghua Lu, Molecular targeted therapy for the treatment of gastric cancer, J. Exp. Clin. Canc. Res. 35 (2016) 1.

[9] M. Arnold, H.E. Karim-Kos, J.W. Coebergh, et al., Recent trends in incidence of five common cancers in 26 European countries since 1988: analysis of the European Cancer Observatory, Eur. J. Canc. 51 (9) (2015) 1164–1187.

[10] J. Ferlay, I. Soerjomataram, R. Dikshit, et al., Cancer incidence and mortality worldwide: sources, methods and major patterns in GLOBOCAN 2012, International Journal of Cancer, 2014.

[11] K. Yuki, I. Masaaki, Y. Kohei, K. Yuki, Y. Naoya, B. Hideo, Update on targeted therapy and immune therapy for gastric cancer, J Cancer Metastasis Treat 4 (2018) 31.

[12] Stomach Cancer, Estimated Incidence, Mortality and Prevalence Worldwide in 2012, Available from: http://globocan.iarc.fr/old/FactSheets/cancers/stomach-new.asp. (Accessed 26 June 2018).

[13] F. Coccolini, E. Cotte, O. Glehen, et al., Intraperitoneal chemotherapy in advanced gastric cancer. Meta-analysis of randomized trials, Eur. J. Surg. Oncol. 40 (2014) 12–26.

[14] F. Lazrak, E.M. Essassi, Y.K. Rodi, K. Misbahi, M. Pierrot, Synthesis of new condensing systems containing 1,2,4-triazole, 1,3-thiazine, 1,3-thiazepine and 1,3,5,7-dithiadiazocine [Synthese de nouveaux systemes condenses renfermant le 1,2,4-triazole, la 1,3-thiazine, la 1,3-thiazepine et la 1,3,5,7-dithiadiazocine, Phosphorus, Sulfur, and Silicon 179 (2004) 1799–1808.

[15] F. Lazrak, N.H. Ahabchane, A. Keita, E.M. Essassi, M. Pierrot, Synthesis and crystal structure of 3-methoxycarbonyl-5-methyl-1-p-tolyl-1,2,4-triazolo [3,4-c]-1,2,4-triazole, Indian J. Chem. B Org. 41 (4) (2002) 821–825.

[16] S. Ming-Xia, D. Xian-Qing, Recent developments on triazole nucleus in anticonvulsant compounds: a review, J. Enzym. Inhib. Med. Chem. 33 (1) (2018) 453–478.

[17] N.K. Basu, F.L. Rose, S-triazolopyridazines: synthesis as potential therapeutic agents, J. Chem. Soc. (1963) 5660.

[18] Gaochan Wu, Yun Gao, Dongwei Kang, Boshi Huang, Zhipeng Huo, Huiqing Liu, Vasanthanathan Poongavanam, Peng Zhan, Xinyong Liu, Design, synthesis and biological evaluation of Tacrine 1,2,3-triazole derivatives as potent cholinesterase inhibitors, Med. Chem. Commun 9 (2018) 149–159.

[19] H. Kumar, A.S. Javed, A.S. Khan, M. Amir, 1,3,4-Oxadiazole/thiadiazole and 1,2,4-triazole derivatives of biphenyl-4-yloxy acetic acid: synthesis and preliminary evaluation of biological properties, Eur. J. Med. Chem. 43 (2008) 2688–2698.

[20] R. Singh, S.K. Kashaw, V.K. Mishra, M. Mishra, V. Rajoriya, V. Kashaw, Design and synthesis of new bioactive 1,2,4-Triazoles, potential antitubercular and antimicrobial agents, Indian J. Pharmaceut. Sci. 80 (1) (2018) 36–45.

[21] M.T.M. El Wassimy, M. Abdel-Rahman, A.B.A.G. Ghattas, O.A.A. Abdallah, Synthesis and reactions of N-Chloromethyl-1,2,4-Triazoles with sulfur and oxygen nucleophiles, phosphorus, Sulfur & Silicon 70 (1992) 99–108.

[22] A.T. Mavrova, D. Wesselinova, J.A. Tsenov, L.A. Lubenov, Synthesis and antiproliferative activity of some new thieno[2,3-d] pyrimidin-4(3H)-ones containing 1,2,4-triazole and 1,3,4-thiadiazole moiety, Eur. J. Med. Chem. 86 (2014) 676–683.

[23] B. Abolghasem, P. Eslam, N. Mehdi, V. Saadat, QSAR modelling of antimalarial activity of urea derivatives using genetic algorithm–multiple linear regressions, J. Saudi Chem. Soc. 20 (3) (2012) 282–290.

[24] E. Pourbasheer, S. Riahi, M.R. Ganjali, P. Norouzi, QSAR study of C allosteric binding site of HCV NS5B polymerase inhibitors by support vector machine, Mol. Divers. 15 (2011) 645–653.

[25] L. Zhong-Hua, Y. Dong-Xiao, G. Peng-Fei, Z. Ji, W. Hao-Ming, H. Biao, G. Qian, Z. Xin-Hui, G. Wen-Ge, Z. Bing, Y. Bin, M. Li-Ying, L. Hong-Min, Design, synthesis and biological evaluation of [1,2,3]triazolo[4,5-d] pyrimidine derivatives possessing a hydrazone moiety as antiproliferative agents, Eur. J. Med. Chem. 124 (2016) 967–980.

[26] L. Zhong-Hua, L. Xue-Qi, Z. Tao-Qian, G. Peng-Fei, G. Wen-Ge, Y. Bin, L. Hong-Min, Design, synthesis and preliminary biological evaluation of new [1,2,3]triazolo[4,5-d]pyrimidine/thiourea hybrids as antiproliferative agents, Eur. J. Med. Chem. 139 (2017) 741–749.

[27] G. Peng-Fei, L. Xue-Qi, Z. Tao-Qian, W. Cong-Cong, L. Zhong-Hua, Z. Ji, W. Hao-Ming, H. Biao, M. Li-Ying, L. Hong-Min, Design, synthesis and in vitro biological evaluation of novel [1,2,3]triazolo[4,5-d]pyrimidine derivatives containing a thiosemicarbazide moiety, Eur. J. Med. Chem. 146 (2018) 147–156.

[28] H. Miao, Y. Jia, S. Xie, X. Wang, J. Zhao, Y. Chu, Z. Zhou, Z. Shi, X. Song, L. Li, Structural insights into the C1q domain of Caprin-2 in canonical Wnt signaling, J. Biol. Chem. 289 (2014) 34104–34113.

[29] Spartan 14, Wave Function, INC, Irvine, CA, 2015.

[30] XLSTAT, Add-in Software (XLSTAT Company), 2009. www.xlstat.com.

[31] M. Ghamali, S. Chtita, A. Ousaa, B. Elidrissi, M. Bouachrine, T. Lakhlifi, QSAR analysis of the toxicity of phenols and thiophenols using MLR and ANN, J. Taibah Univ. Sci. 11 (2017) 1–10.

[32] V.K. Agrawal, P.V. Khadikar, QSAR prediction of toxicity of nitrobenzenes, Bioorg. Med. Chem. 9 (2001) 3035–3040.

[33] A.I. Taourati, M. Ghamali, S. Chtita, H. Zaki, M. Benlyass, F. Guenoun, T. Lakhlifi, M. Bouachrine, QSAR studies of the inhibitory activity of a series of substituted indole and derivatives against isoprenylcysteine carboxyl methyltransferase (icmt), Int. J. Pharmaceut. Sci. Invent. 6 (1) (2017), 06-13.

[34] R.I. Paramita, A. Arsianti, M. Radji, In silico docking studies of alkyl esters derivative of gallic acid on Bcl-xL anti-apoptotic protein of breast cancer, Int. J. Chem. Tech. Res. 10 (1) (2017) 348–355.

[35] H. Rachid, I.T. Abdelhafid, L. Majdouline, A. Azeddine, A. Abdelaziz, B. Mohammed, L. Tahar, Combining DFT and QSAR result for predicting the biological activity of the phenylsuccinimide derivatives, J. Chem. Pharmaceut. Res. 5 (10) (2013) 45–56.

[36] D. Ritchie, D. Kozakov, S. Vajda, Accelerating and focusing protein-protein docking correlations using multi-dimensional rotational FFT generating functions, Bioinformatics 24 (2008) 1865–1873.